

The astronauts worked approximately 22 hr on the lunar surface, traversed about 30 km, collected nearly 120 kg of samples, took more than 2200 photographs, and recorded many direct geologic observations (all lunar records!). The lunar surface data, sample results, and geologic interpretation from orbital photographs are the bases for the following geologic synthesis.

Postmission Interpretation: The Taurus-Littrow massifs are interpreted as the upper part of the thick, faulted ejecta deposited on the rim of the transient cavity of the large southern Serenitatis Basin, which was formed about 3.9 to 4.0 b.y. ago by the impact of a planetesimal. The target rocks, predominantly of the dunite-anorthosite-norite-troctolite suite or its metamorphosed equivalents, were fractured, sheared, crushed, and/or melted by the impact. The resulting mixture of crushed rock and melt was transported up and out of the transient cavity and deposited on and beyond its rim. Hot fragmental to partially molten ejecta and relatively cool cataclastic and relict target rocks were intermixed in a melange of lenses, pods, and veins. Crystallization of melts and thermal metamorphism of fine-grained fragmental debris produced breccia composed of rock and mineral fragments in a fine-grained, coherent, crystalline matrix. Such breccia dominates the massif samples.

High-angle faults that bound the massifs were activated during the formation of the basin, so that structural relief of several kilometers was imposed on the ejecta almost as soon as it was deposited. Massive slumping that produced thick wedges of colluvium on the lower massif slopes probably occurred nearly contemporaneously with the faulting. Material of the Sculptured Hills, probably largely cataclastic excavated from the southern Serenitatis Basin by the same impact, was then deposited on and around the massifs.

Basalt, estimated to be about 1400 m thick at the landing site, flooded the Taurus-Littrow graben before approximately 3.7 b.y. ago. The basalt (subfloor basalt) is part of a more extensive unit that was broadly warped and cut by extensional faults before the accumulation in Mare Serenitatis of younger, less deformed basalts that overlap it. A thin volcanic ash unit (dark mantle), probably about 3.5 b.y. old, mantled the subfloor basalt and the nearby highlands. It, too, was subsequently overlapped by the younger basalt of Mare Serenitatis.

In the time since the deposition of the volcanic ash, continued bombardment by primary and secondary projectiles has produced regolith, which is a mechanical mixture of debris derived mainly from the subfloor basalt, the volcanic ash, and the rocks of the nearby massif and Sculptured Hills. The regolith and the underlying volcanic ash form an unconsolidated surficial deposit with an average thickness of about 14 m, sufficiently thick to permit abnormally rapid degradation of the smaller craters, especially those less than 200 m in diameter, so as to create a surface that appears less cratered than the other mare surfaces. Admixed volcanic ash gives the surface a distinctive dark color, which, in combination with the less cratered appearance, led to its interpretation before the mission as a young dark mantling unit.

The uppermost part of the regolith over much of the landing area is basalt-rich ejecta from the clustered craters of the valley floor. Most of the valley floor craters are interpreted as part of a secondary cluster formed by projectiles of ejecta from Tycho, 2200 km to the southwest. When they struck the face of the South Massif, the projectiles mobilized fine-grained regolith material that was deposited on the valley floor as the light mantle. Exposure ages suggest that the swarm of secondary projectiles struck the Taurus-Littrow area about 100 m.y. ago.

The Lee-Lincoln fault scarp is part of an extensive system of wrinkle ridges and scarps that transect both mare and highland rocks.

The scarp cuts Lara Crater, but the major part of the displacement occurred before the deposition of the light mantle. Small extensional faults cut the surface of the light mantle west of the Lee-Lincoln scarp.

References: [1] Wolfe E. W. et al. (1981) *U.S. Geol. Surv. Prof. Paper 1080*, 280 pp.

N93-1880A308 P-3

THE APOLLO 17 MARE BASALTS: SERENELY SAMPLING TAURUS-LITTROW. Clive R. Neal¹ and Lawrence A. Taylor², ¹Department of Civil Engineering and Geological Sciences, University of Notre Dame, Notre Dame IN 46556, USA, ²Department of Geological Sciences, University of Tennessee, Knoxville TN 37996, USA.

As we are all aware, the Apollo 17 mission marked the final manned lunar landing of the Apollo program. The lunar module (LM) landed approximately 0.7 km due east of Camelot Crater in the Taurus-Littrow region on the south-western edge of Mare Serenitatis [1]. Three extravehicular activities (EVAs) were performed, the first concentrating around the LM and including station 1 approximately 1.1 km south-southeast of the LM at the northwestern edge of Steno Crater [1]. The second traversed approximately 8 km west of the LM to include stations 2, 3, 4, and 5, and the third EVA traversed approximately 4.5 km to the northwest of the LM to include stations 6, 7, 8, and 9. This final manned mission returned the largest quantity of lunar rock samples, 110.5 kg/243.7 lb, and included soils, breccias, highland samples, and mare basalts. This abstract concentrates upon the Apollo 17 mare basalt samples.

One hundred and fifty-six basaltic samples were returned weighing 32.19 kg, or approximately one-third the total weight of Apollo 17 samples. The majority of Apollo 17 mare basalts were found at station 1A (75 samples), 22 from station 0, 19 from station 8, 11 from station 5, 10 from station 6, and 9, 4, 3, 2, and 1 from stations 4, 9, 7, 2, and 3 respectively. Note that these statistics include rake samples, but do not include basaltic clasts from breccia samples (e.g., [2]). Practically all these samples have been studied to various degrees, whether it be just a thin-section cut, to rare-gas, magnetic, isotope, and whole-rock analyses.

Petrographic Studies: The Apollo 17 mare basalts were divided into a three-fold classification on the basis of petrography. The petrographic divisions were derived independently by three different studies [3-5] and the differences between the groups defined by each petrographic study are identical. The petrographic groups are

1. *Type 1A: Olivine porphyritic ilmenite basalts.* These are usually fine-grained (typically <1 mm) with a general subvarioliitic to varioliitic texture, or vitrophyric (e.g., 71157). All type 1A basalts contain olivine and ilmenite phenocrysts (e.g., 71048). Armalcolite, where present, forms cores to ilmenite, is partially rimmed by ilmenite, or is rarely present as discrete grains (up to 0.2 mm; e.g., 71097). Chromite-ulvöspinel is present either as discrete grains (0.1-0.3 mm) or as inclusions in olivine (<0.1 mm). All type 1A basalts contain ilmenites with sawtooth margins, indicative of rapid crystallization (e.g., [3]). Pink pyroxene prisms (≈0.4 mm) and plagioclase laths (≈0.3 mm) are interstitial, sometimes combining to form "bowtie" textures.

2. *Type 1B: Plagioclase-poikilitic ilmenite basalts.* All type 1B basalts are coarse grained (>2 mm), with rare medium-grained examples (e.g., 74287). However, all are olivine poor. In all cases, ilmenite has exsolved both ulvöspinel and rutile, which are present as thin (<0.05 mm wide) lamellae within ilmenite. Armalcolite and discrete chromite-ulvöspinel (0.2-0.5 mm and 0.1-0.2 mm respectively), where present, are inclusions in olivine, pyroxene, and/or

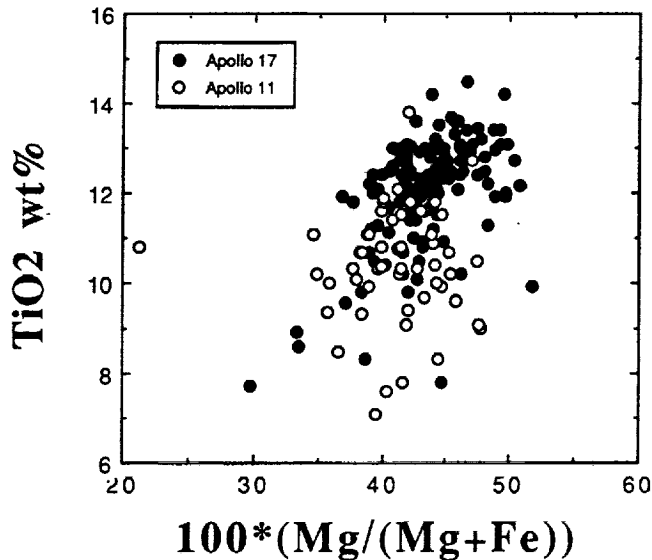


Fig. 1.

plagioclase. Some armalcolites possess a discontinuous ilmenite overgrowth. Where olivine is present, it forms cores to larger pyroxenes or small (up to 0.1 mm) discrete inclusions in plagioclase. It is likely that where olivine is absent, it has been totally resorbed and replaced by pyroxene (e.g., 71047). The petrographic relationships within the type 1B basalts indicate that clinopyroxene (e.g., titan-augite) after olivine. Type 1B basalts commonly contain interstitial SiO_2 , demonstrating the fractionated nature of these basalts.

Type II: Apollo 11, low-K-type basalts. These are olivine-free and have medium-grained (generally 1.5 mm), subophitic textures, similar to the low-K Apollo 11 high-Ti basalts. Subhedral ilmenite is practically the only opaque phase present; it exhibits smooth grain boundaries and contains ulvöspinel and rutile exsolution lamellae (<0.05 mm wide). Interstitial SiO_2 is present (up to 0.6 mm). Unlike the previous groups, type II basalts contain no low-Ca pyroxene.

With regard to mineral species, there is a decrease in modal olivine from type 1A through type II. Ilmenite, armalcolite, and chromite-ulvöspinel tend to be present in similar proportions in both type 1A and type 1B, but type II basalts contain lower modal abundances of these elements. As expected, type 1B basalts generally have higher plagioclase abundances than type 1A; type II basalts have similar plagioclase abundances to type 1B.

Very-low-Ti Basalts: Wentworth et al. [8] described the petrography of Apollo 17 VLT basalts as being granular to subophitic. They consist primarily of pyroxene and plagioclase, with minor olivine and Al-chromite. Pyroxenes range from pigeonite to subcalcic augite, but the majority have pigeonitic compositions. Plagioclase ranges from An_{98} to An_{93} and olivine has a variable composition ($\approx \text{Fo}_{75-58}$).

Whole-Rock Chemistry: Like the Apollo 11 counterparts, 99% of Apollo 17 basalts were originally classified as high Ti [1,7,8], in that they contain >6 wt% TiO_2 , and the remaining 1% are of the very-low-Ti (VLT) subdivision (e.g., [9,10]). However, Apollo 17 high-Ti basalts contain a higher TiO_2 content for a given MG# (Fig. 1), suggesting a higher proportion of Ti-rich minerals in the source region for Apollo 17 high-Ti mare basalts.

Early studies of whole-rock chemistry (e.g., [5,11,12]) subdivided Apollo 17 high-Ti basalts into three groups—A, B, and C. Rhodes et

al. [12] and Warner et al. [11] recognized that data from coarse-grained basalts appeared to plot as clouds about the arrays defined by the fine-grained samples. This scatter was attributed to unrepresentative sampling and were consequently classified as “class U” basalts. It was noted immediately that the three petrographic types did not correspond to the three chemical groups—all three of the former are present in each of the latter.

Apollo 17 type A basalts contain 50–60% higher incompatible trace-element abundances than do the type B variants (Fig. 2), although both possess similar major-element compositions. Neal et al. [13] demonstrated that the type B division contained two subdivisions (B1 and B2) on the basis of REE abundances (Fig. 3). Type C basalts contain higher MgO and Cr_2O_3 abundances than types A, B1, and B2, but are most notable in their enrichment of Rb over the other Apollo 17 high-Ti mare basalts (Fig. 4). The type C basalts have similar incompatible trace-element abundances to the type As. Also, type C basalts contain olivines of the highest Fo content (Fo_{80}) found at Apollo 17, but only five examples have been described [11,12,14], all from station 4 (Shorty Crater). Ryder [15,16] reported the chemistry and petrography of a sample that may be a new variant of Apollo 17 high-Ti basalt (70091,2161), which he classified as type D. This basalt has lower REE abundances, a deeper Eu anomaly (Fig. 2), higher MgO and Cr_2O_3 abundances, and lower CaO and TiO_2 contents than other Apollo 17 high-Ti basalts.

Apollo 17 VLT basalts contain <1 wt% TiO_2 and were first recognized in thin sections from the Apollo 17 deep drill core [9,17], but have since been found in impact melt rocks [18,19] and as basaltic clasts in breccia 73255 and 72235 [2]. However, understanding these basalts is difficult due to small sample size—only a few milligrams of sample have been analyzed for whole-rock chemistry.

The four samples that have been analyzed demonstrate that the VLT basalts contain lower REE abundances than their high-Ti counterparts. In fact, the VLT basalts generally contain lower incompatible trace-element abundances than the high-Ti varieties, but do have slightly higher MG#s (Fig. 1). However, the inherently small sample sizes of these VLT basalts means that interpretation of whole-rock chemistry must proceed with caution.

Isotope Chemistry and Age Dating: Thirty-two published Rb-Sr, Sm-Nd, or ^{40}Ar - ^{39}Ar ages on 17 different Apollo 17 high-Ti basalts have been determined over a period from 1973 to present. Ages range from 3.64 Ga to 3.84 Ga, with the eruption ages of each group

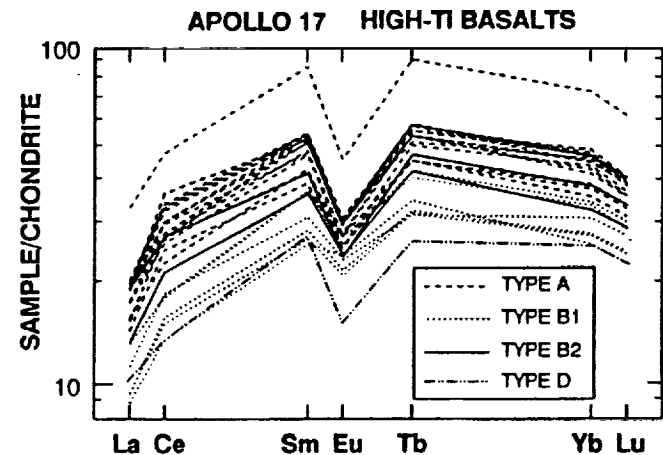


Fig. 2.

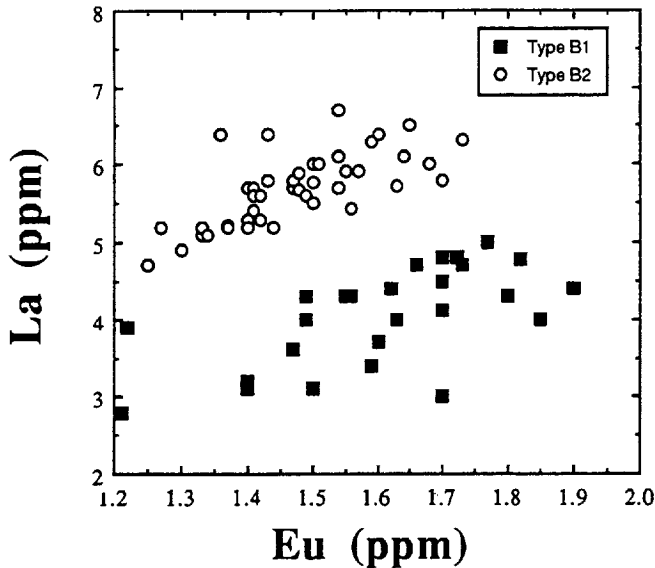


Fig. 3.

being indistinguishable from each other. However, Paces et al. [20] suggested that type A basalts were slightly older (3.75 ± 0.02 Ga) than type B (3.69 ± 0.02 Ga) on the basis of weighted averages of available data. The available age data for type C basalts overlap these two groups and types B1 and B2 are indistinguishable from each other.

An interesting feature of the Apollo 17 high-Ti basalts is that $I(\text{Nd})$ ratios are indistinguishable between the various groups, yet $I(\text{Sr})$ ratios are resolvable between types A, B1, and C [20]. Type B2 basalts appear to have evolved by open-system processes as they exhibit a range in both $I(\text{Sr})$ and $I(\text{Nd})$ [20]. Nyquist et al. [21,22] argued that the range in Rb/Sr between type B (lowest), through type A, to type C (highest) was due to varying degrees of partial melting of slightly heterogeneous sources, with retention of clinopyroxene in the residue. Paces et al. [20] concluded that the Rb/Sr and Sr isotopic heterogeneities were formed at 4.1 Ga by metasomatic processes and clinopyroxene was exhausted during Apollo 17 high-Ti magma genesis. Whatever the process, it is clear that a three-stage model is required to explain the Rb-Sr systematics.

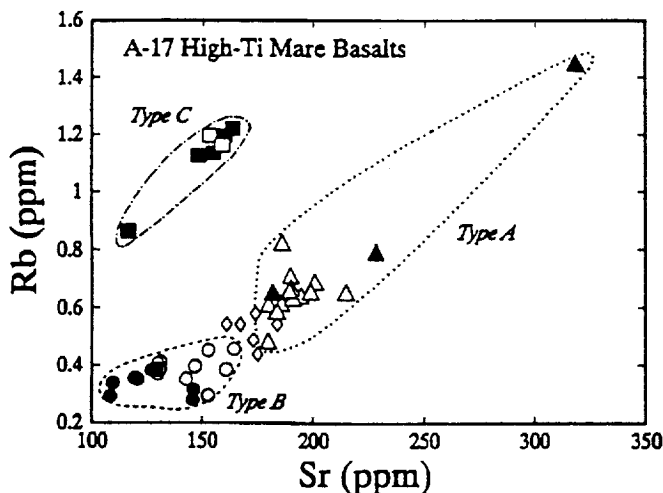


Fig. 4.

Petrogenesis: Rhodes et al. [12] and Warner et al. [11] demonstrated that the type A basalts evolved by closed-system fractional crystallization and proposed that, due to variations of La/Sm ratio, type B basalts could be modeled by varying the degree of partial melting of the source. With the identification of type B1 and B2 basalts [13], it was recognized that on the basis of major and trace elements, both groups could be generated by closed-system fractional crystallization. However, the isotopic study of Paces et al. [20] demonstrated the validity of such a model for the type B1 high-Ti basalts, but identified open-system behavior of the type B2s. Neal et al. [13] also successfully quantified a closed-system fractional crystallization model to the type A basalts. Only five basalts comprise the type C grouping, making quantitative petrogenetic interpretation impossible. Also, the small number of samples and small sample size of the type D and VLT basalts preclude definitive petrogenetic interpretation.

Source Modeling: Apollo 17 high-Ti mare basalts. Source models proposed for these basalts can be divided into those involving (1) early-stage LMO cumulates, (2) late-stage LMO cumulates, and (3) hybridized sources. Isotopic and experimental studies have demonstrated the presence of ilmenite and clinopyroxene in the source region of high-Ti basalts (late-stage LMO cumulates), and the relatively high MG# of these basalts (Fig. 1) requires olivine and/or orthopyroxene (early LMO cumulates). Hughes et al. [23] suggested convective overturn of the LMO cumulate pile in order to account for the chemical composition of the Apollo 17 high-Ti basalt source. Spera [24] stated that LMO-wide overturn was possible, but Snyder et al. [25] considered that the overturn may have been more localized. There are two points of contention about the high-Ti source: (1) Is ilmenite exhausted during partial melting? (2) Is plagioclase in the source?

Apollo 17 VLT mare basalts. Source modeling of the VLT basalts was undertaken by Wentworth et al. [10], who demonstrated that the observed VLT composition could be produced by a 1–2% partial melting of a 90% olivine, 10% orthopyroxene cumulate, assuming that this source crystallized from a LMO with a flat REE profile. These authors further suggested that if this cumulate source formed from a magma with a fractionated REE pattern [e.g., $(\text{La}/\text{Lu})_N \approx 2$], the VLT basalt REE pattern could be generated by $\approx 4\%$ partial melting of 70% olivine, 30% orthopyroxene source mineralogy.

Summary: Two types of mare basalt were returned from the Apollo 17 site: (1) the commonly found high-Ti variety and (2) the rare VLT basalts. The high-Ti basalts were most probably derived from a heterogeneous hybrid source of early and late-stage LMO cumulates. Four, possibly five, groups of basalts were erupted. At least two of these groups evolved through closed-system fractional crystallization and at least one group underwent open-system evolution. Types A, B1, and B2 appear to be present from all over the Taurus-Littrow site, whereas type Cs are only found at station 4 (Shorty Crater) and the extent of the type Ds is not known.

References: [1] *Apollo 17 Lunar Sample Catalog* (1973). [2] James O. B. and McGee J. J. (1980) *Proc. LPSC 11th*, 67–86. [3] Papike J. J. et al. (1974) *Proc. LSC 5th*, 471–504. [4] Brown G. M. et al. (1975) *Proc. LSC 6th*, 1–13. [5] Warner R. D. et al. (1975) *Proc. LSC 6th*, 193–220. [6] LSPET (1973) *Science*, 182, 659–672. [7] Papike J. J. et al. (1976) *Rev. Geophys. Space Phys.*, 14, 475–540. [8] Papike J. J. and Vaniman D. T. (1978) *Mare Crisium: The View from Lunar 24*, 371–402. [9] Vaniman D. T. and Papike J. J. (1977) *Proc. LSC 8th*, 1443–1471. [10] Wentworth S. et al. (1979) *Proc. LPSC 10th*, 207–223. [11] Warner R. D. et al. (1979) *Proc. LPSC 10th*, 225–247.

[12] Rhodes J. M. et al. (1976) *Proc. LSC 7th*, 1467–1489. [13] Neal C. R. et al. (1990) *GCA*, 54, 1817–1833. [14] Neal C. R. et al. (1990) *LPSC XXI*, 855–856. [15] Ryder G. (1988) *Eos*, 69, 292. [16] Ryder G. (1990) *Meteoritics*, 25, 249–258. [17] Taylor G. J. et al. (1977) *GRL*, 4, 207–210. [18] Warner R. D. et al. (1978) *Proc. LPSC 9th*, 547–564. [19] Taylor G. J. et al. (1978) *Mare Crisium: The View from Lunar 24*, 357–370. [20] Paces J. B. et al. (1991) *GCA*, 55, 2025–2043. [21] Nyquist L. E. et al. (1976) *Proc. LSC 7th*, 1507–1528. [22] Nyquist L. E. et al. (1979) *Proc. LPSC 10th*, 77–114. [23] Hughes S. S. et al. (1989) *Proc. LPSC 19th*, 175–188. [24] Spera F. J. (1992) *GCA*, 56, 2253–2265. [25] Snyder G. A. et al. (1992) *GCA*, in press.

2
P
5937-13805 9
USING APOLLO 17 HIGH-TI MARE BASALTS AS WINDOWS TO THE LUNAR MANTLE. Clive R. Neal¹ and Lawrence A. Taylor², ¹Department of Civil Engineering and Geological Sciences, University of Notre Dame, Notre Dame IN 46556, USA, ²Department of Geological Sciences, University of Tennessee, Knoxville TN 37996, USA.

Detailed study of mare basalts and volcanic glasses is critical in our understanding of the lunar mantle because, as yet, no mantle xenoliths have been recognized in the current collection. Primitive endmember, volcanic lunar glass compositions can be considered primary mantle melts because of their glassy, uncrystallized nature, and analyses of such samples yielded important information regarding the mantle source (e.g., [1–3]). The fact that no relationship between the glasses and the crystalline mare basalts has been established suggests that the basalts were derived from a separate source and therefore have the potential to yield further critical information regarding the lunar mantle. By understanding the processes that have occurred during post-magma-generation evolution, parental or possibly primary compositions can be highlighted for further study, possibly leading to source evaluation. However, where it is demonstrable that the composition chosen as the parental/“primary” melt has experienced some post-magma-generation evolution (i.e., a vitrophyre containing olivine/ilmenite/chromite-ulvöspinel phenocrysts), this composition cannot be used for direct calculation of a mantle source. In this case, incompatible trace-element ratios can be utilized to remove the effects of fractional crystallization and allow an evaluation of the source region (e.g., [4,5]).

Apollo 17 Source Modeling: The source composition and location of Apollo 17 high-Ti mare basalts has been under debate for many years and several models have been proposed. The one unifying theme of 99% of these models is that they require a mafic, cumulate mantle source. This is where the similarity ends! Models for titaniferous basalt petrogenesis include those requiring early LMO cumulates of olivine and opx [6], late-stage cumulates [4,7–9], to those requiring a mixture of early and late-stage cumulates [10–15] or hybrid sources [3,16]. Experimental evidence puts the depth of origin of the Apollo 17 high-Ti mare basalts at between 200 and 400 km ([17]; source dominated by olivine and low-Ca pyroxene with ilmenite) to ≤ 150 km [10–12]. The degree of partial melting ranges from 5% to 20%. It is generally agreed that a Fe-Ti oxide mineral is required in the source of Apollo 17 high-Ti mare basalts.

Determination of the depth of origin is critical in understanding the composition, stratigraphy, and dynamics of the lunar mantle. For example, at depths exceeding 300–350 km within the Moon, the source for the high-Ti basalts would be eclogitic [18] and such a source would not yield the inherently LREE-depleted signature of the Apollo 17 high-Ti mare basalts. Therefore, depths must be shallower than 300 km. Furthermore, there are two points of contention in

defining the source regions of Apollo 17 high-Ti mare basalts: (1) Was ilmenite exhausted or retained in the residue? (2) Was plagioclase present in the source? Shih et al. [13] proposed a source composition of olivine + clinopyroxene + ilmenite \pm plagioclase, all of which were retained in the source. On the basis of experimental evidence, Walker et al. [10,11], suggest that ilmenite remains in the residue, and plagioclase, if present, would be exhausted; conversely, Green et al. [17] demonstrate that ilmenite would be exhausted and suggests plagioclase was never present. Hughes et al. [3] conclude that both ilmenite and plagioclase are exhausted from their modeled source composition. Clearly, the nature of the Apollo 17 high-Ti mare basalt source region composition is far from resolved, and the situation is complicated by the recognition of four, possibly five, separate magma types: A, B1, B2, C, and D [19–23].

Recognizing the Apollo 17 High-Ti Mare Basalt Source Region Components: The purpose of this abstract is to use incompatible trace-element ratios to evaluate the nature of the source regions of Apollo 17 type A, B1, B2, and possibly C high-Ti basalts in an attempt to answer the two questions posed above. A database of practically all analyzed Apollo 17 basalts was assembled and the nature of any potential fractionating assemblage evaluated using petrographic observations, coupled with the MAGMAFOX program of Longhi [24]. Samples chosen for processing by the MAGMAFOX program were either fine grained or vitrophyric. The results demonstrate a fractionating sequence dominated by chromite-ulvöspinel, olivine, ilmenite, and pyroxene (low and high Ca). Plagioclase becomes a liquidus phase only after $\approx 55\%$ crystallization. As demonstrated by Neal et al. [21], over 98% of all types A, B1, and B2 can be modeled by 40% closed-system fractional crystallization of olivine, chromite-ulvöspinel, armalcolite, ilmenite, and augite. This assemblage is generally supported by the MAGMAFOX program, except for armalcolite (calculated as ilmenite), and the program results also include pigeonite. Therefore, because plagioclase is not part of the fractionating assemblage, Sm and Eu can be considered as incompatible elements, as are La, Yb, and Hf. Although ilmenite is fractionating, the Hf crystal/liquid partition coefficient for ilmenite is ≈ 0.4 [25]. As part of this study, the Yb/Hf ratio is used because although both are incompatible (i.e., $K_d < 1$), these elements will have approximately the same partition coefficient value in the fractionating assemblage described above. Significant changes in this ratio will

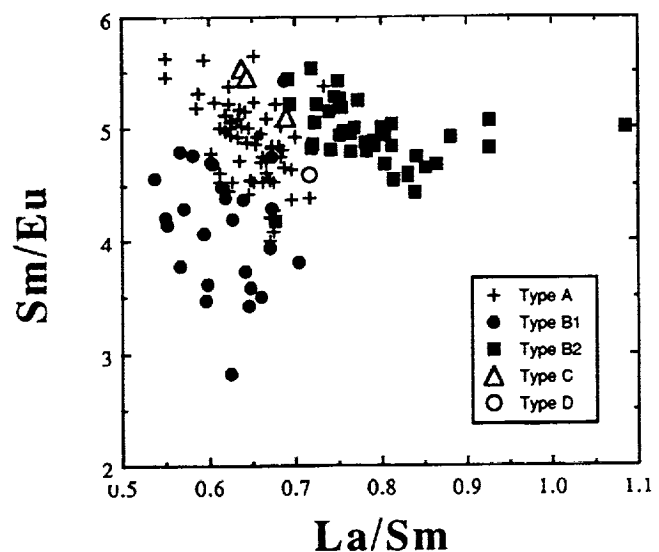


Fig. 1.